11-23-2005

Modeling Gas Holdup in Gas–Liquid–Fiber Semibatch Bubble Columns

Xuefeng Su
Iowa State University

Theodore J. Heindel
Iowa State University, theindel@iastate.edu

Modeling Gas Holdup in Gas−Liquid−Fiber Semibatch Bubble Columns

Xuefeng Su and Theodore J. Heindel*

Department of Mechanical Engineering, Iowa State University, Ames, Iowa 50011-2161

Three gas holdup models are developed that correspond to different flow regimes in a 15.24-cm-diameter semibatch bubble column filled with various fiber suspensions. Three different perforated plate aerators are used and have open area ratios (A) of 0.57%, 0.99%, and 2.14%. Rayon fiber suspensions with lengths (L) of 3, 6, and 12 mm and cellulose fibers are used to form the fiber suspensions over a range of fiber mass fractions up to 1.8%. The models reproduce most of the data within ±15%. A limitation of the current models, due to limited experimental data, is that the model coefficients and exponents vary with aeration plate open area ratio and column diameter.

Introduction

One area of gas−liquid−solid bubble column research that has gained recent attention is gas−liquid−fiber (GLF) bubble columns, where the solid phase is a flexible fiber. GLF systems are found in the pulp and paper industry in many unit operations including paper recycling (i.e., flotation deinking), fiber bleaching, direct-contact steam heating, and deaeration.

Fiber suspensions can be described as complex fluids because unique flow characteristics result when the fibers are flexible, have a large aspect ratio, and have a density close to that of water. Fiber−fiber interactions result in fiber flocculation. Fiber mass (volume) fraction, aspect ratio (ratio of fiber length to diameter), and type influence fiber floc formation, size, and strength. The combination of these factors can be represented by the crowding number (N).[1] When $N \leq 1$, fiber−fiber contact occurs only occasionally, and fibers are free to move; when $1 < N < 150$, flocs can appear in the suspension, and fiber mobility decreases.

Yield stress is an important characteristic in fiber suspension rheology. Fiber concentration, aspect ratio, length distribution, and type have an impact on the suspension yield stress.[2,3] The yield stress is also affected by gas holdup when gas flows through a fiber suspension.[4] Suspension yield stress can also produce a significant effect on gas flow behavior in a fiber suspension, assist fiber flocs in trapping bubbles, and produce channeling phenomenon at high fiber mass fractions. Fiber−fiber interactions are also important to the effective fiber suspension viscosity. Sundararajakumar and Koch[5] showed that the effective fiber suspension viscosity increases nonlinearly with $N_f L^3$, where N_f is the number of fibers per unit volume. Other factors such as fiber flexibility, shape, and friction coefficient also affect fiber flocculation, yield stress, and suspension viscosity.[6]

The resulting fiber suspension characteristics lead to a very complex suspension rheology, which has a significant effect on bubble behavior. Thus, factors that affect fiber suspension characteristics also influence gas holdup in fiber suspensions.

* To whom correspondence should be addressed. E-mail: theindel@iastate.edu. Fax: 515-294-3261.

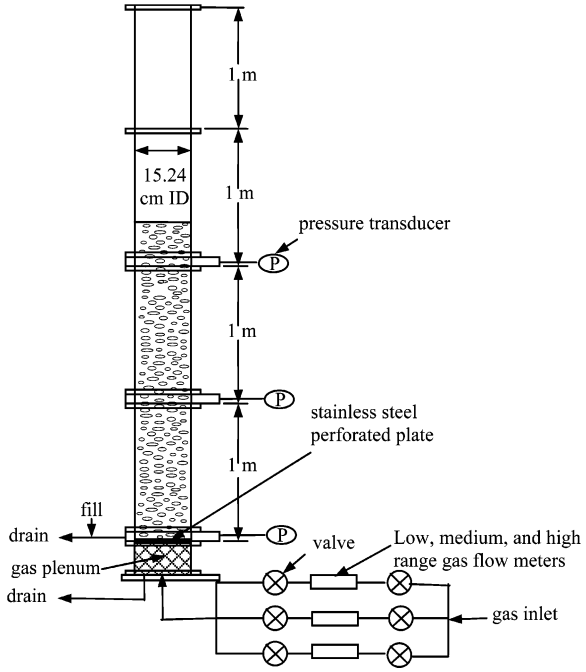

Figure 1. Experimental bubble column.

Gas holdup in fiber suspensions has been studied.[7−14] These studies show that fiber mass fraction and type have significant effects on gas holdup. To date, however, little work has been done on gas holdup model development in fiber suspensions. This paper addresses this void and develops models to reproduce gas holdup in gas−liquid−fiber semibatch bubble columns. These models are the first step in providing predictive tools for gas−liquid−fiber flows.

Experimental Procedures

The bubble column experimental facility used in this study is schematically represented in Figure 1. The bubble column consists of four 1-m sections of 15.24-cm-i.d. cast acrylic, yielding a total column height of 4 m. Gas is injected at the base of the column through one of three stainless steel perforated plates with open areas (A) of 0.57%, 0.99%, and 2.14%. Details of these plates can be found in Su and Heindel.[14] A gas plenum

10.1021/ie050816e CCC: $30.25
Published on Web 10/29/2005

Table 1. Cellulose Fiber Properties

	hardwood	softwood	BCTMP[a]
wood species	eucalyptus	65−75% northern black spruce, 20−25% jackpine, 5−10% balsam fir	northern pine
particle average fiber length (mm)	0.69	1.2	0.8
length-weighted average fiber length (mm)	0.78	2.31	1.91
coarseness (mg/100 m)	6.9	13.1	29.5
number of fibers per gram (millions)	21.4	6.37	4.25

[a] Bleached chemithermomechanical pulp.

is located below the perforated plate and is filled with glass beads to promote a uniform gas distribution into the test facility. Three mass flowmeters are used to measure the gas flow rate to encompass a low, medium, and high gas flow rate ranges. Three pressure transducers are installed along the column, one located at the column base, one at a column height from the perforated plate (H) of 1 m, and one at a height of 2 m. The mass flowmeters and pressure transducers are interfaced to a data acquisition system. Average gas flow rates and pressures are recorded from 4000 individual readings sampled at a frequency of 200 Hz.

The gas holdup is determined from the column pressure drop. In a semibatch system, the frictional pressure drop is negligible, so the total pressure drop corresponds to the hydrostatic head; in this case,

$$\epsilon = 1 - \frac{\Delta P}{\Delta P_0} \tag{1}$$

where ΔP is the difference between the average local pressure at any two pressure transducers with superficial gas velocities (U_g) > 0, and ΔP_0 is the corresponding average value with $U_g = 0$. For gas−liquid (GL) systems, ΔP_0 equals the liquid hydrostatic head; for GLF systems, ΔP_0 corresponds to the fiber slurry hydrostatic head.

The fibers studied in this paper include rayon fiber with lengths (L) of 3, 6, and 12 mm and fiber diameters (d_f) of 20.6 μm, which are used with all three aeration plate open area ratios, and cellulose fibers [i.e., softwood, hardwood, bleached chemithermomechanical pulp (BCTMP)], which are used only with the open area ratio of 0.57%. The characteristics of the cellulose fibers are provided in Table 1.Various fiber mass fractions ($0 \le C \le 1.8\%$) and superficial gas velocities ($U_g \le 18$ cm/s) are investigated. The superficial liquid velocity in this study is held constant at 0. The gas used in all experiments is filtered compressed air. The percent uncertainty in the superficial gas velocity measurements is estimated to be ±2−4%, and the absolute uncertainty in the gas holdup is estimated to be $\Delta\epsilon = \pm 0.006-0.008$. More details of the experimental procedures can be found in Su and Heindel[14] and Su.[15]

Experimental Results

Typical trends of the effect of the fiber mass fraction on the gas holdup using three different gas aeration plates (A = 0.57%, 0.99%, and 2.14%) are shown in Figure 2 for 3-mm-long rayon fibers.[14] For all three aeration plates, the gas holdup decreases with increasing fiber mass fraction. This phenomenon is attributed

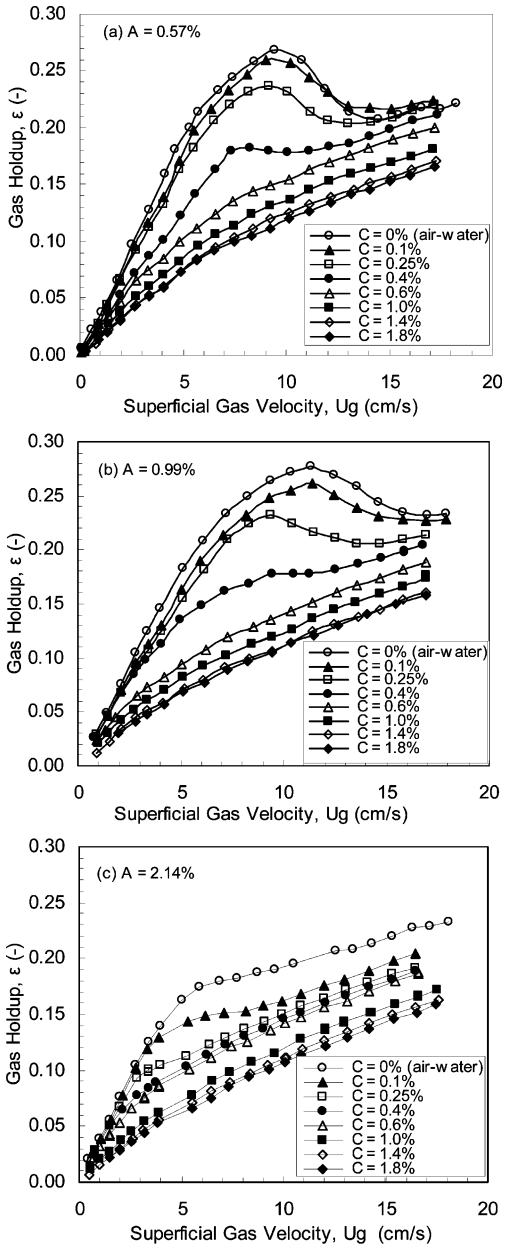

Figure 2. Effect of fiber mass fraction on gas holdup with different aeration plates for 3-mm-long rayon fiber suspensions:[14] A = (a) 0.57%, (b) 0.99%, and (c) 2.14%.

to the promotion of bubble coalescence and/or reduction of bubble breakup due to the increase in the effective suspension viscosity with increasing fiber mass fraction and the increase in the large bubble size due to the increasing yield stress of the fiber suspension, as has been explained by Su and Heindel.[12] The trends in the gas holdup variation with fiber mass fraction for A = 0.57% and 0.99% are similar. At low fiber mass fractions ($C \le 0.4\%$, Figure 2a,b), the gas holdup behavior is similar to that of an air−water system: there is a maximum gas holdup, indicating that homogeneous, transitional, and heterogeneous flow regimes exist over the range of superficial gas velocities. The effect of the fiber mass fraction is more significant in the transitional flow regime, whereas little influence is observed in the homogeneous flow regime. At $C > 0.4\%$, the gas holdup continuously increases with increasing superficial gas velocity, and pure heterogeneous flow, as defined by Ruzicka et al.,[16] is observed.

For $A = 2.14\%$ (Figure 2c), the gas holdup increases monotonically with increasing superficial gas velocity for all fiber mass fractions. At low fiber mass fractions ($C \leq 0.25\%$), a homogeneous flow regime exists at low superficial gas velocities, and when $C > 0.25\%$, pure heterogeneous flow appears over the range of superficial gas velocities. Similar trends are obtained for rayon fiber with $L = 6$ and 12 mm for all three aeration plates. More details can be found in Su and Heindel.[14]

Factors Influencing Gas Holdup. Fiber type, mass fraction, length, flexibility, shape, and friction coefficient influence fiber flocculation, yield stress, and effective suspension viscosity,[1,2,6,17,18] and these factors can also affect gas holdup in fiber suspensions. However, fiber stiffness, friction coefficient, and shape are difficult to measure and control, and they depend, to some extent, on fiber origin (e.g., type) and processing conditions.[19] Only fiber type, mass fraction, and length are considered in this gas holdup model development. Note that, in the models below, superficial gas velocity, fiber length, and fiber mass fraction are in units of meters per second, meters, and percent, respectively.

According to the definition of the crowding number (N)[1]

$$N = 5\frac{CL^2}{\omega} \tag{2}$$

where C is the fiber mass fraction (in percent), L is the fiber length (in mm), and ω is the fiber coarseness (in kg/m). The crowding number accounts for the effect of fiber mass fraction and length on fiber flocculation; hence, it will be used to replace fiber mass fraction and length in the models.

The crowding number, however, is not able to uniquely describe the effect of fiber mass fraction and length on gas holdup. Su and Heindel[12] showed that the same crowding number for different fiber suspensions does not produce the same gas holdup, and this phenomenon is attributed to the fact that the crowding number exaggerates the effect of fiber length on gas holdup, especially when the fibers are long. Su[15] argued that it might be more appropriate to combine the crowding factor with another (other) quantity (quantities) to describe the fiber effect on gas holdup.

Fiber number density (N_f), with units of number of fibers per unit volume, has been used by some researchers to account for the effect of fiber concentration on yield stress and suspension viscosity.[3,5] N_f is expressed as

$$N_f = \frac{\rho_w \frac{C}{100}}{\frac{d_f^2}{4}\pi L \rho_f} \tag{3}$$

for rayon fiber and

$$N_f = n_f \frac{C}{100}\rho_{eff} \tag{4}$$

for cellulose fiber, where n_f is the number of fibers per gram of oven-dry material, C is the fiber mass fraction in percent, and ρ_{eff} is the effective fiber suspension density. The values of n_f for the cellulose fibers in this study are provided in Table 1.

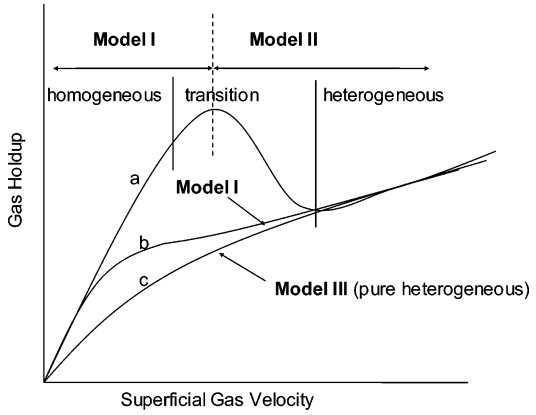

Figure 3. Gas holdup models for different flow regimes.

For fibers with a uniform diameter such as rayon, N_f is proportional to C/L (eq 3). Thus, the combination of N_f with N reduces the effect of the fiber length and enhances the effect of the fiber mass fraction.

Model Development. Three models are developed to encompass all hydrodynamic conditions of this study. According to Figure 2, gas holdup as a function of superficial gas velocity follows three general flow regime trends, depending on the fiber mass fraction and aeration plate open area. Figure 3 summarizes the three types of gas holdup patterns as a function of superficial gas velocity over the entire range of fiber mass fractions. Two of the flow patterns exhibit three-regime flow (homogeneous, transitional, and heterogeneous flow), one with and one without a local maximum gas holdup, whereas the third flow pattern follows pure heterogeneous flow. The three-regime flow and pure heterogeneous regime are considered separately.

For the three-regime flow, it is shown in Figure 2 that, for $A = 0.57\%$ and 0.99%, there is a local maximum gas holdup with increasing superficial gas velocity, and this local maximum divides the transitional flow regime into two parts: The first part is characterized by increasing gas holdup with increasing superficial gas velocity, and the second part is characterized by decreasing gas holdup with increasing superficial gas velocity; for $A = 2.14\%$, no local maximum gas holdup appears. Therefore, for $A = 0.57\%$ and 0.99%, two different methods are used to deal with these two gas holdup behaviors (as shown in Figure 3): Model I describes the homogeneous flow and the first part of the transitional flow regime, and model II describes the second part of the transitional flow and heterogeneous flow regime. Model I is also used for the entire three-regime flow for $A = 2.14\%$ (i.e., it is applicable when homogeneous flow is initially observed at low gas flow rates and as long as gas holdup increases with increasing superficial gas velocity). Model III is developed for pure heterogeneous flow for all three open area ratios. The individual models do not account for the effect of the open area ratio. Su and Heindel[14] showed that the gas holdup is not a monotonic function of the open area ratio and that there is a critical open area ratio that generates a maximum gas holdup. However, there are only three open area ratios in the current study, and they do not provide enough information to determine an exact mathematic description of the open area ratio effect. Hence, models I, II, and III have different coefficients and exponents for different open area ratios.

Table 2. Fiber Mass Fraction (%) Ranges within Which Three-Regime Flow Occurs

	rayon fiber L (mm)					
open area ratio (A) (%)	3	6	12	hardwood	softwood	BCTMP
0.57	$C < 0.6$	$C < 0.4$	$C < 0.4$	$C < 0.6$	$C < 0.4$	$C < 0.6$
0.99	$C < 0.6$	$C < 0.4$	$C < 0.4$	–	–	–
2.14	$C < 0.6$	$C < 0.4$	$C < 0.25$	–	–	–

Three-Regime Flow. Three-regime flow exists when the fiber mass fraction is low. The critical fiber mass fraction at which the flow pattern changes from three-regime flow to pure heterogeneous flow differs for different open area ratios and fiber lengths. The fiber mass fraction ranges within which three-regime flow is observed are summarized in Table 2; these ranges become narrower with increasing fiber length and weakly depend on the open area ratio.

Model I: Homogeneous Flow and the First Part of the Transitional Flow Regime (A = 0.57% and 0.99%). Based on a force balance on bubbles bubbling through a bubble column, Mersmann[20] derived a gas holdup correlation in a dilute bubble swarm. This model assumed that bubble motion was in a quasisteady state, and hence, the velocity of the bubble in a swarm was determined by the balance of the buoyant and drag forces

$$C_d \frac{\pi d_b^2}{4} \frac{\rho_c v_r^2}{2} = \frac{\pi d_b^3}{6} \Delta\rho_d g \tag{5}$$

where C_d is the bubble drag coefficient in a swarm, d_b is the bubble diameter, v_r is the relative bubble velocity, ρ_c is the density of the continuous phase, and $\Delta\rho_d$ is the density difference between the mixture (gas and liquid) and the gas.

In the present study, ρ_c is the effective fiber−water slurry density (ρ_{eff}), and $\Delta\rho_d$ is the density difference between the gas−liquid−fiber mixture and the gas. Additionally, v_r and $\Delta\rho_d$ are

$$v_r = \frac{U_g}{\epsilon} \tag{6}$$

for a semibatch bubble column and

$$\Delta\rho_d = \rho_m - \rho_g = (1-\epsilon)(\rho_{eff} - \rho_g) = (1-\epsilon)\Delta\rho \tag{7}$$

where ρ_m is the density of the gas−liquid−fiber system and can be calculated as

$$\rho_m = \epsilon\rho_g + (1-\epsilon)\rho_{eff} \tag{8}$$

Substituting eqs 6 and 7 into eq 5 and rearranging yields

$$\epsilon(1-\epsilon)^{1/2} = c\left(\frac{C_d}{d_b}\right)^{1/2} U_g \tag{9}$$

where

$$c = \left(0.75\frac{\rho_{eff}}{\Delta\rho g}\right)^{1/2}$$

In the present study, fiber addition has a negligible effect on the overall slurry density, so c is assumed to be constant.

On the basis of other researchers' experimental data, Mersmann[20] suggested a more exact expression obtained by the following modification of eq 9

$$\epsilon(1-\epsilon)^n = c\left(\frac{C_d}{d_b}\right)^{1/2} U_g \tag{10}$$

The exponent n depends on the density ratio of the continuous phase to the dispersed phase. When the ratio is greater than 200, $n = -4$. This agrees with the results of Akita and Yoshida.[21] For the present study, the continuous phase can be assumed to be a homogeneous water−fiber slurry, and the dispersed phase is air. For these conditions, the density ratio is greater than 200, so $n = -4$ for this model.

Mersmann[20] also discussed in detail the fact that both C_d and d_b are functions of fluid properties, such as the surface tension, viscosity, and difference in density between the two phases. For the experimental conditions in the present study, it is assumed that, in these three quantities, only the effective viscosity varies with fiber addition. The effective viscosity depends on fiber type, mass fraction, length, shear rate, and superficial gas velocity.[22−24]

In addition, yield stress has an important effect on bubble diameter. The bubble diameter is required to be large enough to produce enough buoyant force to break through the fiber network.[12,25,26] Thus, bubble diameter is a function of fiber type, mass fraction, and length because of their effects on yield stress.

The combination of N and N_f is employed to replace the fiber mass fraction and length and account for the effect of the fiber on the drag coefficient and bubble diameter. The influence on the bubble diameter is visually apparent; increasing the fiber mass fraction (i.e., increasing N and N_f) increases the bubble diameter.[27,28] Additionally, Hebrard et al.[29] observed that the bubble diameter depends on the superficial gas velocity and that the relationship is related to the gas distributor type. They determined that, for a perforated plate gas distributor (which is the case in the present study), the bubble diameter decreases with increasing U_g.

On the basis of the above analysis, the quantity C_d/d_b is a function of U_g, N_f, and N. Hence, eq 10 can be rewritten as

$$\frac{\epsilon}{(1-\epsilon)^4} = f(U_g, N_f, N)U_g \tag{11}$$

Su[15] found that the combination $N^a N_f^b$ is a reliable parameter for describing the effects of fiber mass fraction and fiber length and proposed a gas holdup model in the form

$$\frac{\epsilon}{(1-\epsilon)^4} = a_1 U_g^{a_2} N^{a_3} N_f^{a_4} \tag{12}$$

The coefficient a_1 and exponents a_2−a_4 in eq 12 are

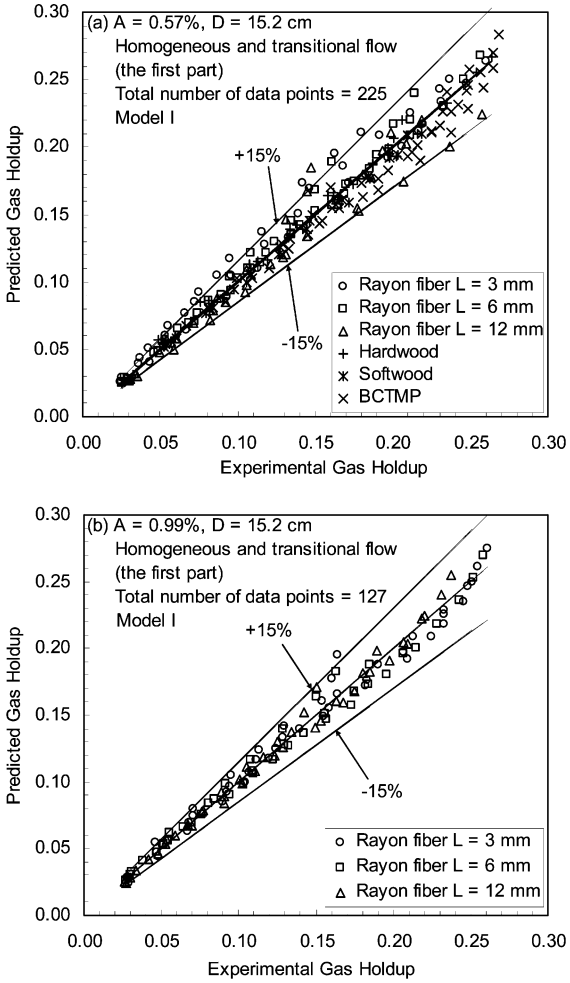

Figure 4. Comparison of the experimental gas holdup values with those predicted using (a) eq 13 for $A = 0.57\%$ and (b) eq 14 for $A = 0.99\%$.

determined by nonlinear curve-fitting tools in MATLAB. The resulting gas holdup correlations are

$$\frac{\epsilon}{(1-\epsilon)^4} = 40.5 U_g^{1.4} N^{-0.146} N_f^{-0.006} \quad \text{(model I} - A = 0.57\%) \quad (13)$$

and

$$\frac{\epsilon}{(1-\epsilon)^4} = 183.7 U_g^{1.289} N^{-0.128} N_f^{-0.106} \quad \text{(model I} - A = 0.99\%) \quad (14)$$

Figure 4 compares the predicted results with the experimental data and reveals that 94% (214 of 225) and 98.4% (125 of 127) of the data can be reproduced within ±15% for $A = 0.57\%$ and 0.99%, respectively. Equations 13 and 14 show that the exponents of N and N_f are negative, indicating that gas holdup decreases with increasing N and N_f. This is consistent with the physical mechanism: the larger N and N_f, the larger the viscosity and yield stress, which leads to a larger bubble diameter and higher bubble rise velocity, resulting in a smaller gas holdup.

Model I: Homogeneous, Transitional, and Heterogeneous Flows (A = 2.14%). For this open area ratio, there is no maximum gas holdup over the range of superficial gas velocities investigated. It is convenient that all three flow regimes are considered in one model. Although model I is based on the assumption of a quasisteady state, Mersmann[20] argued that the resulting expression for gas holdup is applicable to heterogeneous flow. Akita and Yoshida[21] applied a correlation similar to that of Mersmann[20] to a wide range of superficial gas velocities encompassing homogeneous and heterogeneous flow. In addition, the good agreement of the predictions with experimental data for this study, as shown in Figure 5, indicates that this model is also applicable to heterogeneous flow.

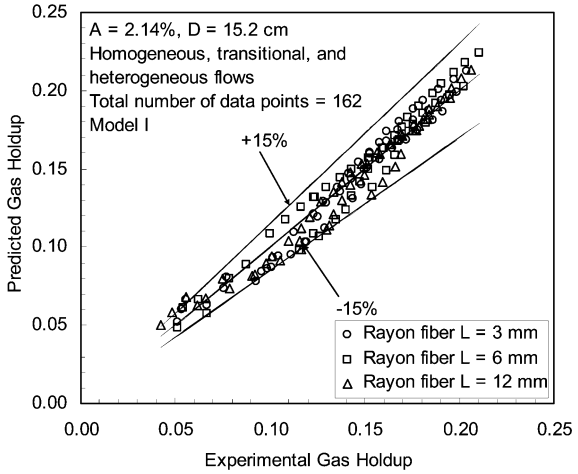

Figure 5. Comparison of the experimental gas holdup values with those predicted using eq 15 for $A = 2.14\%$.

By fitting the data to eq 12 with the nonlinear curve fitting package in MATLAB, the gas holdup correlation for three-regime flow with $A = 2.14\%$ is found to be

$$\frac{\epsilon}{(1-\epsilon)^4} = 26.52 U_g^{0.781} N^{-0.11} N_f^{-0.11} \quad \text{(model I}, A = 2.14\%) \quad (15)$$

Figure 5 compares the predicted gas holdup and experimental data; 96% (155 of 162) of the data are reproduced within ±15% using eq 15.

Equation 15 shows that, at a given superficial gas velocity, the gas holdup decreases with increasing N and N_f for the range of superficial gas velocities investigated. It is noted that gas holdup depends on U_g to a power less than 1 instead of greater than 1 (i.e., eqs 13 and 14), which indicates that the increase in gas holdup with increasing superficial gas velocity is less when $A = 2.14\%$ than when $A = 0.57\%$ or 0.99%. This is evident in Figure 2 and can be attributed to the fact that, for $A = 2.14\%$, bubbles tend to coalesce near the distribution plate with increasing U_g because of the small hole spacing, resulting in an increased probability of bubble–bubble interactions with adjacent bubbles.[14]

Model II: Heterogeneous and the Second Part of the Transitional Flow Regime (A = 0.57% and 0.99%). After a maximum gas holdup is reached when $A = 0.57\%$ and 0.99%, a local minimum gas holdup is observed before heterogeneous flow is reached. For these conditions, when $U_g/(1-\epsilon)$ is plotted as a function of U_g for various fiber mass fractions, a straight line results (Figure 6).

Figure 6 also shows that, for each open area ratio, the difference among slopes is negligible, but the intercepts change with different fiber lengths and mass

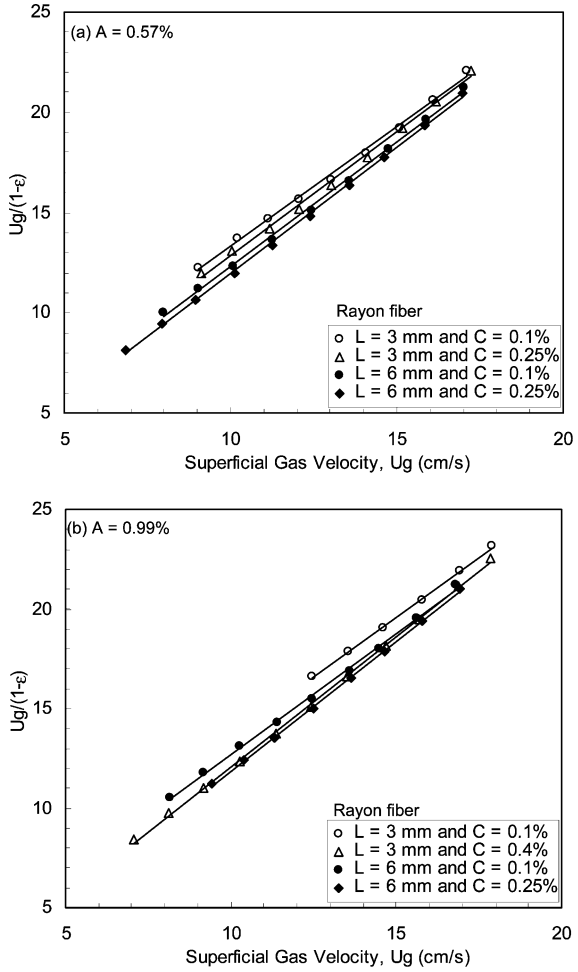

Figure 6. $U_g/(1-\epsilon)$ as a function of superficial gas velocity for different fiber lengths and mass fractions with A = (a) 0.57% and (b) 0.99%.

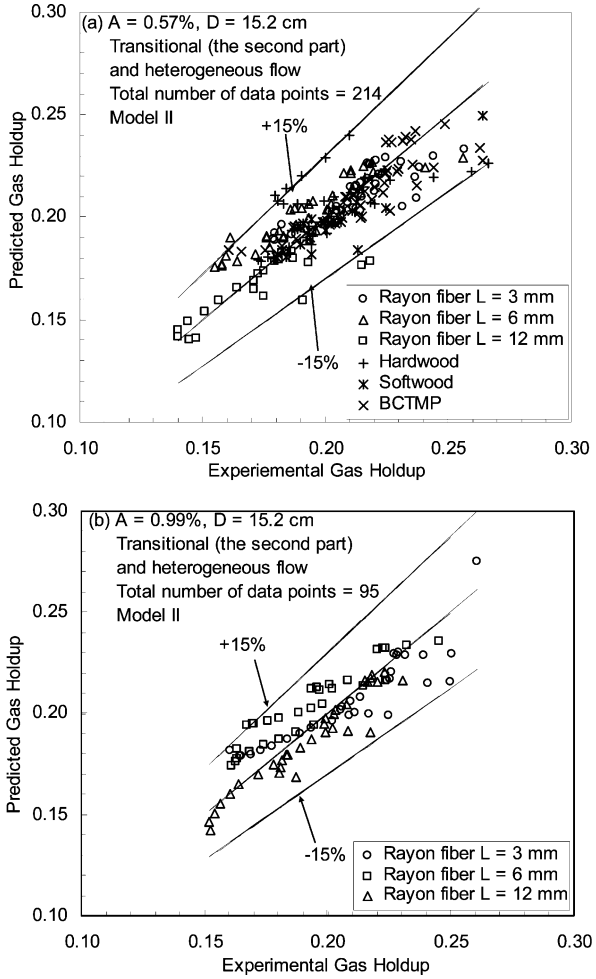

Figure 7. Comparison of predicted and experimental data of the second part of transitional and heterogeneous flows for A = (a) 0.57% and (b) 0.99%.

fractions. Therefore, the correlation for this regime is assumed to be

$$\frac{U_g}{(1-\epsilon)} = a_1 U_g + f(C,L) \tag{16}$$

As with model I, N and N_f are used to account for the effect of C and L. Su[15] plotted $f(C,L)$ as a function of the parameter $N^a N_f^b$ and determined, through trial and error, that $f(C,L)$ is well described by $\ln(N^a N_f^b)$. Additionally, to generalize $U_g/(1-\epsilon)$, U_g is assumed to vary as a power function. Hence, the correlation for the second part of the transitional flow and the heterogeneous flow regime for A = 0.57% and 0.99% is proposed to be

$$\frac{U_g}{(1-\epsilon)} = a_1 U_g^{a_2} + \ln(N^{a_3} N_f^{a_4}) + a_5 \tag{17}$$

The coefficients a_1 and a_5 and exponents a_2–a_4 for A = 0.57% and 0.99% are listed in Table 3.

Figure 7 shows that the model can reproduce 97% (207 of 214) of the data within ±15% for A = 0.57% and 99% (93 of 94) data within ±15% for A = 0.99%.

Pure Heterogeneous Flow. Model III: Pure Heterogeneous Flow Regime (A = 0.57%, 0.99%, and 2.14%). Model III is used to describe the flow when pure heterogeneous flow is observed at all superficial gas velocities, and it is based on the Zuber–Findlay drift flux model.[30] The drift flux model considers the mixture as a whole and reduces the difficulties associated with interface interactions. For a semibatch bubble column, the drift flux is expressed as

Table 3. Coefficients and Exponents in Model II Eq 17 for A = 0.57% and 0.99%

	A = 0.57%	A = 0.99%
a_1	1.617	1.469
a_2	1.209	1.1267
a_3	−0.0039	−0.0039
a_4	−0.0013	−0.0026
a_5	0.0648	0.0817

$$\frac{U_g}{\epsilon} = C_0 U_g + V_{0j} \tag{18}$$

where U_g/ϵ represents the mean gas velocity. The distribution parameter, C_0, is constant for a specified flow pattern and reflects the nonuniformity in flow and gas holdup profiles. For uniform flow, C_0 = 1. However, in general, C_0 depends on the flow regime, pressure, channel geometry, and flow rate.[31] Kataoka et al.[32] pointed out that C_0 is larger in semibatch systems than in systems in which the liquid velocity is nonzero and high, and the drift velocities are almost the same for both liquid velocity conditions.

Zuber and Findlay[30] argued that V_{0j} represents the terminal bubble rise velocity for heterogeneous flow and

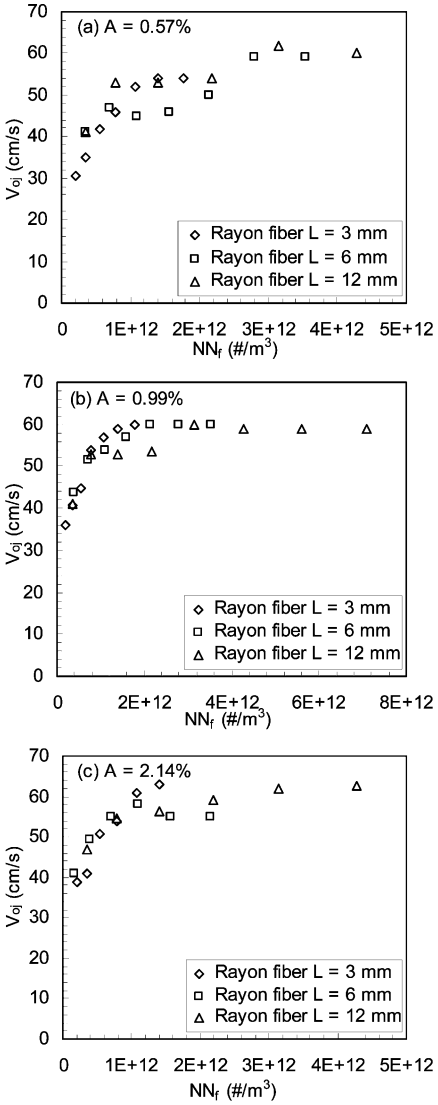

Figure 8. Terminal bubble rise velocity as a function of the product of N and N_f for A = (a) 0.57%, (b) 0.99%, and (c) 2.14%.

that the value is independent of bubble size. In this model, V_{0j} is called the terminal bubble rise velocity. For heterogeneous flow, the plot of the mean gas velocity (U_g/ϵ) as a function of U_g is a straight line whose slope represents C_0 and whose intercept is the terminal bubble rise velocity.

Su[15] determined that C_0 can be approximated as a constant for different fiber lengths and fiber mass fractions for all values of $A = 0.57\%$, 0.99%, and 2.14% and that the terminal bubble rise velocity is a function of fiber mass fraction and length and increases with increasing fiber mass fraction for all three fiber lengths. When the fiber mass fraction is high, terminal bubble rise velocity varies only slightly with fiber mass fraction.

On the basis of the above analysis, the gas holdup model for this flow regime can be assumed to be

$$\frac{U_g}{\epsilon} = C_0 U_g + g(C,L) \tag{19}$$

where $g(C,L)$ represents the terminal bubble rise velocity V_{0j}. It is assumed that $g(C, L)$ can be described by a functional relationship involving N and N_f,[15] i.e.

$$V_{0j} = g'(N,N_f) \tag{20}$$

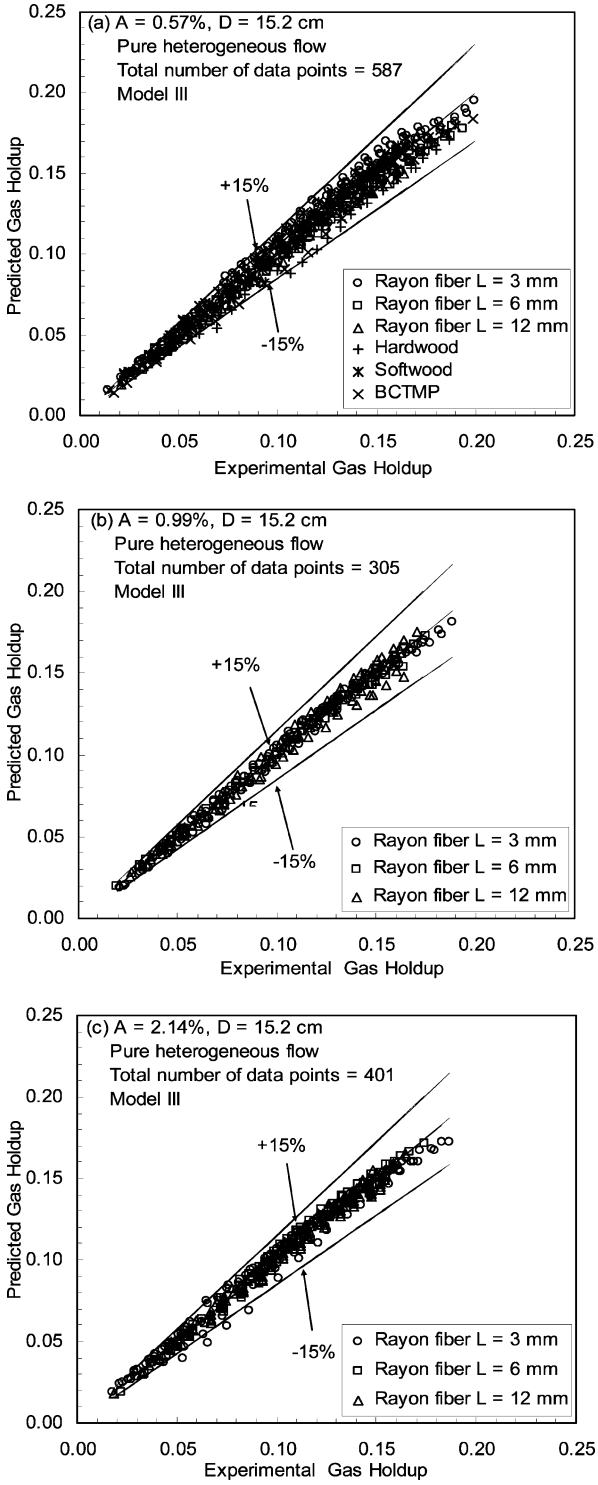

Figure 9. Comparison of predicted gas holdup to experimental data for pure heterogeneous flow for A = (a) 0.57%, (b) 0.99%, and (c) 2.14%.

Table 4. Coefficients and Exponents of Model III Eq 21 for A = 0.57%, 0.99%, and 2.14%

	$A = 0.57\%$	$A = 0.99\%$	$A = 2.14\%$
C_0	3.0	3.11	3.13
C_1	0.078	0.069	0.057
C_2	0.044	0.074	0.053
C_3	−0.917	−1.50	−0.958

Terminal bubble rise velocities for different fiber mass fractions and lengths are plotted as a function of $N^a N_f^b$ ($a = b = 1$ for all three open area ratios by trial and

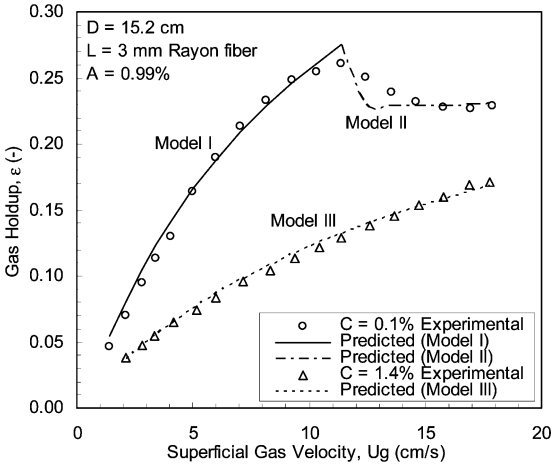

Figure 10. Comparison between predictions and experimental data at specified fiber mass fractions for rayon fiber (L = 3 mm) and A = 0.99%.

error) in Figure 8. The terminal bubble rise velocities for each open area ratio converge to a single line and follow a logarithmic function. Therefore, the gas holdup model for pure heterogeneous flow is proposed to be of the form

$$\frac{U_g}{\epsilon} = C_0 U_g + \ln(N^{C_1} N_f^{C_2}) + C_3 \qquad (21)$$

Table 4 lists the coefficients and exponents of eq 21 for all pure heterogeneous flow conditions of this study.

From Table 4, the values of the distribution parameter C_0 for all three open area ratios are very similar, indicating that, when the fiber mass fraction is high, the influence of the open area ratio on the gas holdup distribution is negligible. This implies that, for suspensions with high fiber mass fractions, bubble behavior is weakly dependent on the aeration plate and mainly depends on slurry mixing.

Figure 9 shows a comparison of the predicted gas holdup values with experimental data for A = 0.57%, 0.99%, and 2.14%. It is shown that the model reproduces 99% (581 of 587) of the data for A = 0.57%, 100% (305 of 305) of the data for A = 0.99%, and 99% (397 of 401) of the data for A = 2.14% within ±15%.

Model Evaluation. The three models are plotted with representative data in Figure 10 for 3-mm-long rayon fiber and an open area ratio of 0.99%. At low fiber mass fractions (C = 0.1%), three-regime flow is observed, and models I and II are used to describe the entire range of results. Model I does a good job of reproducing the data from the homogeneous regime to the first part of the transition regime. The latter part of the transition regime is difficult to capture, with model II reproducing the observed trends, but not necessarily the data. Model II does much better at high superficial gas velocities, where the flow is heterogeneous. At higher fiber mass fractions (e.g., C = 1.4%), where the flow is purely heterogeneous, model III reproduces the data over the entire range of superficial gas velocities.

The models that were developed above for a 15.2-cm semibatch bubble column have been extended to data obtained in a 32.1-cm-i.d. semibatch bubble column with a perforated plate gas distributor with A = 0.49%.[33] Su[15] showed that the models work very well provided that the coefficients are altered to account for column diameter effects; more details are provided elsewhere.[15]

Conclusions

Three basic gas holdup models were developed for gas−liquid−fiber semibatch bubble columns operating in (i) the homogeneous flow regime and the first part of the transitional flow regime (A = 0.57% and 0.99%) and the entire range of three-regime flow (A = 2.14%), (ii) the second part of the transitional flow regime and the heterogeneous flow regime (A = 0.57% and 0.99%), and (iii) the pure heterogeneous flow regime (A = 0.57%, 0.99%, and 2.14%). The models reproduced most of the data within ±15% for the bubble column used in this study (D = 15.2 cm). A significant limitation of the models, due to limited experimental data, is that the model coefficients and exponents vary with different bubble column diameters and open area ratios; thus, the current models cannot be used for scale-up. However, they are a good first step in developing comprehensive gas holdup models for fiber suspensions.

A parameter in the gas holdup models, $N^a N_f^b$, reliably accounted for the complex effect of fiber type, fiber mass fraction, and fiber length. The exponents a and b were functions of the bubble column flow regime, open area ratio, and column diameter.

Acknowledgment

Financial support of this work by the National Science Foundation under Grant CTS-0209928 is greatly appreciated. The cellulose fiber was supplied and characterized by Kimberly−Clark Corporation; their support is appreciated.

Nomenclature

a_i = coefficients in eqs 11 and 16
A = open area ratio, %
c = constant in eq 9
C = fiber mass fraction, %
C_d = bubble drag coefficient in a swarm
C_0 = drift flux model constant
d_b = bubble diameter, mm
d_f = fiber diameter, μm
L = fiber length, mm or m in models
n_f = number of fibers per gram of oven-dry material, number/g
N_f = number of fibers per unit volume, number/m^3
N = crowding number
P = average pressure of the air−water−fiber suspension, Pa
P_0 = average pressure of the water−fiber suspension, Pa
U_g = superficial gas velocity, cm/s or m/s in models
V_{0j} = average drift velocity or terminal bubble rise velocity, cm/s
v_r = relative bubble rise velocity

Greek Letters

ϵ = gas holdup
ρ_{eff} = effective density of the fiber-water mixture, kg/m^3
ρ_g = gas density, kg/m^3
ρ_f = dry fiber density, kg/m^3
ρ_w = water density, kg/m^3
ρ_c = density of the continuous phase
ω = fiber coarseness, kg/m
Δ = difference

Literature Cited

(1) Kerekes, R. J.; Schell, C. J. Characterization of Fiber Flocculation Regimes by a Crowding Factor. *J. Pulp Paper Sci.* **1992**, *18*, J32.

(2) Bennington, C. P. J.; Kerekes, R. J.; Grace, J. R. The Yield Stress of Fiber Suspensions. *Can. J. Chem. Eng*. 1990, *68*, 748.

(3) Andersson, S. R.; Ringner, J.; Rasmuson, A. The Network Strength of Non-Flocculated Fiber Suspensions. *Nord. Pulp Paper Res.* **1999**, *14*, 61.

(4) Bennington, C. P. J.; Azevedo, G.; John, D. A.; Birt, S. M.; Wolgast, B. H. The Yield Stress of Medium-Consistency and High-Consistency Mechanical Pulp Fiber Suspensions at High Gas Contents. *J. Pulp Paper Sci.* **1995**, *21*, J111.

(5) Sundararajakumar, R. R.; Koch, D. L. Structure and Properties of Sheared Fiber Suspensions with Mechanical Contacts. *J. Non-Newtonian Fluid Mech.* **1997**, *73*, 205.

(6) Joung, C. G.; Phan-Thien, N.; Fan, X. J. Viscosity of Curved Fibers in Suspension. *J. Non-Newtonian Fluid Mech.* **2002**, *102*, 1.

(7) Went, J.; Jamialahmadi, M.; Muller-Steinhagen, H. Effect of Wood Pulp Fiber Concentration on Gas Holdup in Bubble Column. *Chem. Ing. Tech.* **1993**, *63*, 306.

(8) Lindsay, J. D.; Ghiaasiaan, S. M.; Abdel-Khalik, S. I. Macroscopic Flow Structures in a Bubbling Paper Pulp−Water Slurry. *Ind. Eng. Chem. Res.* **1995**, *34*, 3342.

(9) Schulz, T. H.; Heindel, T. J. A Study of Gas Holdup in Cocurrent Air/Water/Fiber System. *Tappi J.* **2000**, *83*, 58.

(10) Xie, T.; Ghiaasiaan, S. M.; Karrila, S.; McDonough, T. Flow Regimes and Gas Holdup in Paper Pulp−Water−Gas Three-Phase Slurry Flow. *Chem. Eng. Sci.* **2003**, *58*, 1417.

(11) Janse, P.; Gomez, C. O.; Finch, J. A. Effect of Pulp Fibers on Gas Holdup in a Flotation Column. *Can. J. Chem. Eng.* **1999**, *77*, 22.

(12) Su, X.; Heindel, T. J. Gas Holdup in a Fiber Suspension. *Can. J. Chem. Eng.* **2003**, *81*, 412.

(13) Su, X.; Heindel, T. J. Gas Holdup Behavior in Nylon Fiber Suspensions. *Ind. Eng. Chem. Res.* **2004**, *43*, 2256.

(14) Su, X.; Heindel, T. J. Effect of Perforated Plate Open Area on Gas Holdup in Rayon Fiber Suspensions. *ASME J. Fluids Eng.* 2005, *127*, 816.

(15) Su, X. Gas Holdup in a Gas−Liquid−Fiber Semi-Batch Bubble Column. Ph.D. Thesis, Iowa State University, Ames, Iowa, 2005.

(16) Ruzicka, M. C.; Zahradnik, J.; Drahos, J.; Thomas, N. H. Homogeneous−Heterogeneous Regime Transition in Bubble Columns. *Chem. Eng. Sci.* **2001**, *56*, 4609.

(17) Schmid, C. F.; Switzer, L. H.; Klingenberg, D. J. Simulations of Fiber Flocculation: Effects of Fiber Properties and Interfiber Friction. *J. Rheol.* **2000**, *44*, 781.

(18) Switzer, L. H.; Klingenberg, D. J. Flocculation in Simulations of Sheared Fiber Suspensions. *Int. J. Multiphase Flow* **2004**, *30*, 67.

(19) Smook, G. A. *Handbook for Pulp & Paper Technologists*, 2nd ed.; Angus Wilde Publications: Bellingham, WA, 1992.

(20) Mersmann, A. Design and Scale-up of Bubble and Spray Columns. *Ger. Chem. Eng.* **1978**, *1*, 1.

(21) Akita, K.; Yoshida, F. Gas Holdup and Volumetric Mass-Transfer Coefficient in Bubble Columns—Effects of Liquid Properties. *Ind. Eng. Chem. Process Des. Dev.* **1973**, *12*, 76.

(22) Joung, C. G.; Phan-Thien, N.; Fan, X. J. Direct Simulation of Flexible Fibers. *J. Non-Newtonian Fluid Mech.* **2001**, *99*, 1.

(23) Shamlou, P. A.; Rajarajan, J.; Ison, A. P. Gas Holdup, Liquid Circulation Velocity and Shear Rate in an External Loop Airlift Containing Non-Newtonian Polymer Solutions. *Bioprocess Eng.* **1998**, *19*.

(24) Al-Masry, W. Effect of Scale-up on Average Shear Rates for Aerated Non-Newtonian Liquids in External Loop Airlift Reactors. *Biotechnol. Bioeng.* **1999**, *62*, 494.

(25) Walmsley, M. R. W. Air Bubble Motion in Wood Pulp Fiber Suspension. *Appita J.* **1992**, *45*, 509.

(26) Pelton, R.; Piette, R. Air Bubble Holdup in Quiescent Wood Pulp Suspensions. *Can. J. Chem. Eng.* **1992**, *70*, 660.

(27) Heindel, T. J. Bubble Size Measurements in a Quiescent Fiber Suspension. *J. Pulp Paper Sci.* **1999**, *25*, 104.

(28) Heindel, T. J.; Garner, A. E. The Effect of Fiber Consistency on Bubble Size. *Nord. Pulp Paper* Res. **1999**, *14*, 171.

(29) Hebrard, G.; Bastoul, D.; Roustan, M. Influence of the Gas Sparger on the Hydrodynamic Behavior of Bubble Columns. *Chem. Eng. Res. Des.* **1996**, *74*, 406.

(30) Zuber, N.; Findlay, J. D. Average Volumetric Concentration in Two Phase Flow Systems. *ASME J. Heat Transfer* **1965**, *87*, 453.

(31) Wallis, G. B. *One-Dimensional Two-Phase Flow*; McGraw-Hill: New York, 1969.

(32) Kataoka, Y.; Suzuki, H.; Murase, M. Drift-Flux Parameters for Upward Gas Flow in Stagnant Liquid. *J. Nucl. Sci. Technol.* **1987**, *24*, 580.

(33) Hol, P. Gas Holdup in a 32 cm Bubble Column. M.S. Thesis, Iowa State University, Ames, Iowa, 2005.

Received for review July 12, 2005
Revised manuscript received September 8, 2005
Accepted September 29, 2005

IE050816E